The solution of Eq. (7) is given by

$$Z = [-\alpha \pm (\alpha^2 - \beta)^{1/2}]\, r^2 \tag{8}$$

It can be shown that $\alpha^2 > \beta$. Therefore, Z is a real quantity.

To facilitate the ensuing discussion of stability, Eq. (6) is recast in the following form:

$$\xi^2 - 2[1 + (Z/2)]\xi + 1 = 0 \tag{9}$$

In order for the error not to grow with increasing time, $|\xi|$ must be less than or equal to one. This condition requires that

$$|1 + (Z/2)| \leq 1 \tag{10}$$

Equations (8) and (10) may be combined to yield

$$-4 \leq [-\alpha \pm (\alpha^2 - \beta)^{1/2}]\, r^2 \leq 0 \tag{11}$$

Since the right-hand inequality is always satisfied for all values of r, one needs consider only the left-hand inequality. Furthermore, one needs consider only the conservative case, namely:

$$[\alpha + (\alpha^2 - \beta)^{1/2}]\, r^2 \leq 4$$

which in turr yields

$$\Delta t \leq 2\Delta x/[\alpha + (\alpha^2 - \beta)^{1/2}]^{1/2} \tag{12}$$

In order to assure a stable numerical calculation, it is useful to determine an upper bound for r, or the largest time increment permissible for a selected space mesh size. This is accomplished by substituting the maximum possible value of α in Eq. (12). The following equation is obtained as a result:

$$\Delta t \leq \frac{2\Delta x}{\left(4(a/b) + (c/2b)(\Delta x)^2 + \{[4(a/b) + (c/2b)(\Delta x)^2]^2 - 64D/b\}^{1/2}\right)^{1/2}} \tag{13}$$

If the value of β in Eq. (12) is taken to be zero, the following simple result is obtained:

$$\Delta t \leq \frac{\Delta x}{[2(a/b) + (c/4b)(\Delta x)^2]^{1/2}} \tag{14}$$

In terms of the plate properties Eq. (14) becomes

$$\Delta t \leq \left\{\frac{\rho(1 - \nu^2)/E}{2 + (1/12)(1 - \nu)\pi^2[1 + (3/2)(\Delta x/h)^2]}\right\}^{1/2} \Delta x \tag{15}$$

When a combination of time increment and space mesh sizes satisfies Eqs. (13) or (15), the calculation of the transient response of a moderately thick plate will be stable. However, Eq. (15) constitutes a more stringent condition than Eq. (13). It may be used for a rough estimate. When the amount of computing time becomes of primary concern, Eq. (13) should be used instead. For a constant space mesh size, Eqs. (13) and (15) indicate that when the plate thickness becomes smaller, the allowable time increment also becomes smaller. Although the classical plate theory can be deduced from the improved plate theory in an analytical way, Eqs. (13) and (15) impose a limitation on the applicability of the latter in the numerical solution of a thin plate under dynamic loads. This is due to the fact that for a relatively thin plate the time increment (for a constant space mesh size) must be kept sufficiently small to avoid any numerical instability. Therefore, as a result, a larger amount of computing time is required. It should be commented here that Eqs. (13) and (15) may also be used as the stability criterion for the calculation of transient response of moderately thick shells to dynamic loads. The reason for this possible extension has been given in Ref. 3.

Reduction to the Thin Plate Case

The stability condition for the finite-difference equation for a thin plate cannot be directly deduced from that for a moderately thick plate, i.e., Eqs. (13) and (15). This is because the latter has been derived by the consideration of the branch of roots of Eq. (9) represented by the case where the sign in front of $(\alpha^2 - \beta)^{1/2}$ in Eq. (11) is negative. This branch contains the higher frequencies of vibration of the discrete system which does not exist in the equation for a thin plate. These frequencies become infinite as the plate thickness approaches zero. To obtain the stability condition for a thin plate, one can examine the second branch of the roots which is given by the case where the sign in front of $(\alpha^2 - \beta)^{1/2}$ in Eq. (11) is positive. After making use of the fact that $\beta/\alpha^2 \ll 1$ for a thin plate and by using the same reasoning in obtaining Eq. (13), it can be shown that

$$\Delta t \leq \tfrac{1}{4}(\rho h/D)^{1/2}(\Delta x)^2 \tag{16}$$

Equation (16) is the same as Eq. (10) in Leech's paper.[1] In contrast to Eqs. (13) and (15), Eq. (16) indicates that for a constant space mesh size, the allowable time increment becomes larger as the plate thickness becomes smaller.

Effect of Transverse Shear or Rotary Inertia

It is interesting to note that when either the effect of transverse shear or rotatory inertia is included, the sufficient stability condition is identical to that for the thin plate. This result can be derived in a similar manner. The actual derivation will not be given here in the interest of brevity.

References

[1] Leech, J. W., "Stability of Finite-Difference Equations for the Transient Response of a Flat Plate," *AIAA Journal*, Vol. 3, No. 9, Sept. 1965, pp. 1772–1773.

[2] Mindlin, R. D., "Influence of Rotatory Inertia and Shear on Flexural Motions of Isotropic, Elastic Plates," *Journal of Applied Mechanics*, Vol. 18, No. 1, March 1951, pp. 31–38.

[3] Leech, J. W., "Finite-Difference Calculation Method for Large Elastic-Plastic Dynamically Induced Deformations of General Thin Shells," AFFDL TR 66-171, Dec. 1964, Air Force Flight Dynamics Lab., Wright-Patterson Air Force Base, Ohio.

Analysis of Coaxial Free Mixing Using the Turbulent Kinetic Energy Method

P. T. Harsha* and S. C. Lee†
ARO Inc., Arnold Air Force Station, Tenn.

Nomenclature

C = concentration of jet species
D = nozzle diameter
H = total enthalpy
k = turbulent kinetic energy per unit mass

Received December 4, 1970; revision received May 3, 1971. This research was performed under the provisions of U.S. Air Force Contract F40600-71-C-0002 with ARO Inc., the operating contractor of the Arnold Engineering Development Center (AEDC) for the Air Force Systems Command. Major financial support was provided by the Air Force Office of Scientific Research under Air Force Project 9711. Project monitor was B. T. Wolfson. Further reproduction is authorized to satisfy the needs of the U.S. Government.

Index category: Jets, Wakes, and Viscid-Inviscid Flow Interactions.

* Research Engineer, J-Division Special Projects Section, Engine Test Facility. Member AIAA.

† Consultant; Associate Professor, Department of Mechanical and Aerospace Engineering, University of Missouri at Rolla, Rolla, Mo. Member AIAA.

Pr_k = Prandtl number for turbulent kinetic energy
Pr_t = turbulent Prandtl number for mean flow energy
r = radial coordinate
Sc_t = turbulent Schmidt number for jet species
u = axial component of mean velocity
u' = axial component of turbulent velocity fluctuation
v = lateral component of mean velocity
v' = lateral component of turbulent velocity fluctuation
w' = tangential component of turbulent velocity fluctuation
x = axial coordinate

Subscripts

ρ = density
c = center line value
j = value at jet exit
o = value in surrounding stream
$\langle\ \rangle$ = indicates time average

Introduction

THE turbulent kinetic energy method for the analysis of free turbulent mixing rests on a fairly general empirical relationship that exists between the turbulent shear stress and the turbulent kinetic energy in a variety of turbulent flows.[1] With this relationship, the turbulent shear stress can be treated as an additional dependent variable to be obtained by a simultaneous solution of the turbulent kinetic energy equation with the other governing equations of the flow. As is discussed in Ref. 2, the system of equations describing a flow may be made either parabolic or hyperbolic, depending on the form chosen for the diffusion term in the turbulent kinetic energy equation. The hyperbolic system was used by Bradshaw et al.[3] for the solution of the wall boundary-layer problem, and it has recently been extended to inhomogeneous free mixing flows by Laster.[4] Lee and Harsha[2] have demonstrated the application of the parabolic form of the turbulent kinetic energy equation to some simple free mixing flows. This Note describes the extension of the method of Ref. 2 to more complex free mixing flows, including mass and energy transfer.

Analysis

The governing equations for coaxial free mixing can be written in parabolic form if the turbulent fluxes are represented by eddy diffusivities. In addition to the continuity, momentum, and kinetic energy equations, written as Eqs. (7, 8, and 11) of Ref. 2, respectively, solution of a problem including simultaneous momentum, mass, and energy transfer requires the solution of the following two equations:

$$\rho u\left(\frac{\partial H}{\partial x}\right)+\rho v\left(\frac{\partial H}{\partial r}\right)=r^{-1}\left(\frac{\partial}{\partial r}\right)\left\{\rho\epsilon Pr_t^{-1}\left[\left(\frac{\partial H}{\partial r}\right)+(Pr_tPr_k^{-1}-1)\left(\frac{\partial k}{\partial r}\right)+(Pr_t-1)\partial\left(\frac{u^2/2}{\partial r}\right)\right]\right\} \quad (1)$$

and concentration (for a two-component mixture with no reactions)

$$\rho u\left(\frac{\partial C}{\partial x}\right)+\rho v\left(\frac{\partial C}{\partial r}\right)=r^{-1}\left(\frac{\partial}{\partial r}\right)\left[\rho\epsilon r Sc_t^{-1}\left(\frac{\partial C}{\partial r}\right)\right] \quad (2)$$

The form of the governing equations is that given by Patankar and Spalding.[5] The variable ϵ appearing in these equations is defined by the expression $\rho\epsilon = \tau/(\partial u/\partial r)$ where the turbulent shear stress τ is obtained from the turbulent kinetic energy equation through the use of an empirical relation[1,2]

$$\tau = a_1\rho k \quad (3)$$

in which k, the turbulent kinetic energy, is given by $k = \frac{1}{2}\langle u'^2 + v'^2 + w'^2\rangle$. The parameter ϵ, which corresponds to the kinematic eddy viscosity, is not itself modeled in this method, but is only evaluated as an intermediate step in the calculation. Its introduction is necessary to retain the parabolic character of the system of equations.[2] The dissipation term in the kinetic energy equation is taken to be the same as that used in Ref. 2, with the length scale l taken to be the mixing layer width in the first (potential core) regime and twice the half-velocity radius $r_{1/2}$ in the second regime (downstream of the potential core). Here, $r_{1/2}$ is the radius at which $u = u_o + \frac{1}{2}(u_c - u_o)$. Finally, the radial variation of the parameter a_1 is taken to be the same as that used for the axisymmetric flow in Ref. 2; that is,

$$a_1 = 0.3(\partial u/\partial r)/|\partial u/\partial r|_{\max} \quad (4)$$

from the center line to the radius at which $\partial u/\partial r = (\partial u/\partial r)_{\max}$ and

$$a_1 = 0.3(\partial u/\partial r)/|\partial u/\partial r| \quad (5)$$

for the remainder of the profile. Although crude, Eqs. (4) and (5) can be shown to closely approximate the experimental behavior of the ratio $\tau/\rho k$, at least in the fully-developed region of jets and wakes. The numerical technique used is a modification of that developed by Patankar,[5] as described in Ref. 2. In all calculations, the dissipation constant $a_2 = 1.5$ and $Pr_k = 0.7$.

Results

Constant-density air-air mixing

The first application is to constant density coaxial mixing, represented by the data of Forstall[6] for $u_o/u_j = 0.25$. In this experiment a helium tracer was used to investigate mass transfer. The presence of this tracer gas was neglected in the calculation reported here. Thus, for this application, only the continuity, momentum, and turbulent kinetic energy equations were used. The calculations were begun at $x = 0$ using the initial shear layer thicknesses presented by Forstall in his thesis[6] with an assumed $\frac{1}{7}$ power law velocity profile. The initial turbulent shear stress profile needed for the kinetic energy calculation was generated using the Prandtl eddy viscosity model.[7] The center line velocity decay results of this calculation are shown in Fig. 1, along with a calculation made using the same numerical technique but with the Prandtl model used to evaluate the turbulent shear stress throughout the flow. In the latter case the constant used in the Prandtl model was taken to be 0.007 in the first regime and 0.011 in the second, as recommended by Peters.[8] As can be seen from Fig. 1, the results of the kinetic energy calculation compare quite favorably with those obtained with the Prandtl model in predicting the length of the near field; clearly the kinetic energy method is superior in the far field.

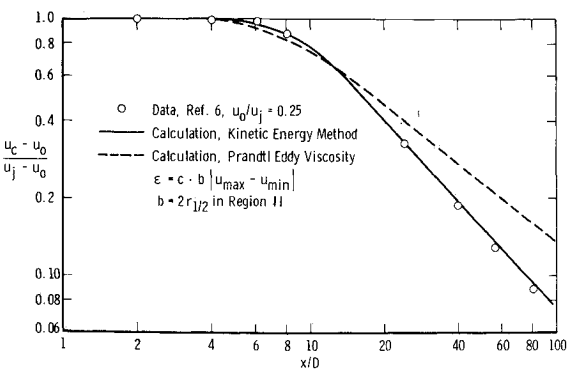

Fig. 1 Comparison of kinetic energy method with Prandtl eddy viscosity calculation for constant-density coaxial mixing.

Variable-density air-air mixing

The coaxial mixing data of Paulk[9,10] includes flows with small temperature differences (approximately 10%) between the streams. Two of these flows were selected for com-

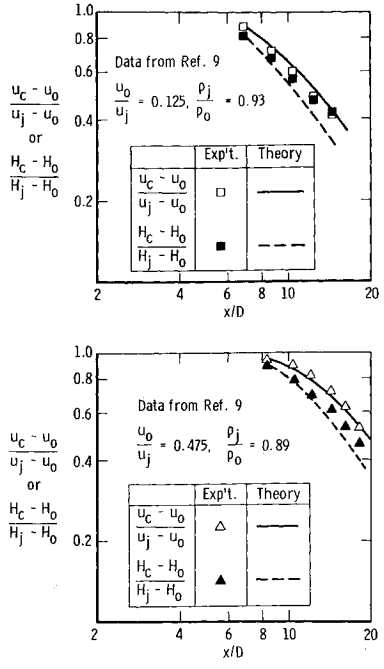

Fig. 2 Comparison of centerline decay predictions of kinetic energy method with experimental data, variable-density coaxial mixing.

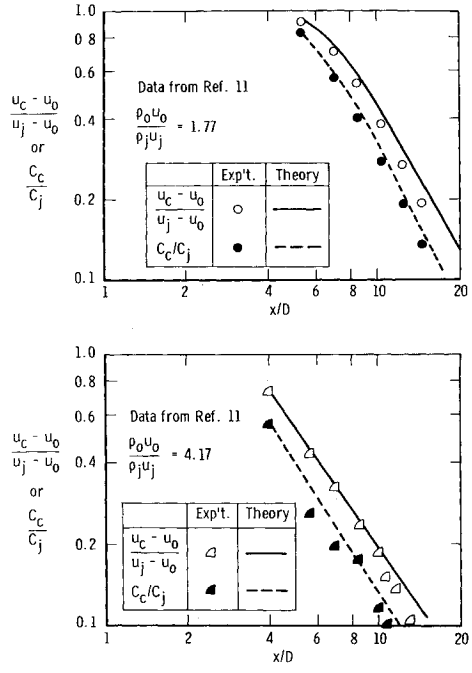

Fig. 3 Comparison of centerline decay predictions of kinetic energy method with experimental data, coaxial hydrogen-air mixing.

parisons with the predictions of the turbulent kinetic energy method. For these calculations the mean energy equation was included, with the turbulent Prandtl number taken to be 0.60 consistent with the data of Ref. 9. The constants used in the kinetic energy analysis were the same as used for the constant-density data of Forstall. Because the experimental data do not include detailed initial profiles, these calculations were begun downstream of the origin at the first axial position for which reliable shear stress profiles (obtained using the integrated form of the axial momentum equation[10]) were available. Results comparing the calculated axial decay of center line velocity ratio and enthalpy ratio with the experimental data for these quantities are shown in Fig. 2. The agreement can be seen to be very good.

Coaxial hydrogen-air mixing

For the nonreactive hydrogen-air system, the energy and species concentration equations are both used. The data of Chriss[10,11] were chosen for comparison, as these include shear stress profiles. For these data, the turbulent Prandtl number was experimentally found to be 0.85[10] as was the turbulent Schmidt number. These values were used in the calculations, which again used the same values of the constants in the kinetic energy equation. Calculations of two of the cases reported by Chriss are shown here; the results are typical of the results obtained with this method for the remainder of these data. Both calculations were begun downstream of the potential core at the first axial station for which there was reliable turbulent shear stress data, which Chriss obtained in the same manner as Paulk. Calculated axial decays of center line velocity ratio and composition are shown on Fig. 3 along with the experimental data for these quantities. Once again the agreement is quite good. Of particular interest is the fidelity with which the kinetic energy method reproduces the slope of the velocity and composition decay curves.

Conclusions

The calculations described in this note demonstrate the remarkable accuracy of the kinetic energy method when applied to a wide range of different coaxial mixing flows, using the same set of constants in the kinetic energy equation for all calculations. This accuracy is obtained at the cost of an increased complexity of initial conditions in that the turbulent shear stress (or turbulent kinetic energy) profile must be known to start the calculation. However, if the history of the turbulence does play an important role in the development of a turbulent flowfield, then clearly a description of the initial profile of the turbulent shear stress is necessary for the proper computation of it. The calculations shown here have demonstrated that given a knowledge of these initial conditions, the turbulent kinetic energy method can produce excellent results in a variety of flowfields. The calculation of the constant-density data of Forstall has shown that if the initial shear stress level is correctly described, excellent results can be obtained with the kinetic energy method using initial turbulent shear stress profiles obtained with a locally-dependent eddy viscosity model. However, experience has shown that this method cannot be recommended in general. There is a clear need for further research into methods of specifying initial turbulent shear stress profiles for use with the turbulent kinetic energy equation.

References

[1] Harsha, P. T. and Lee, S. C., "Correlation Between Turbulent Shear Stress and Turbulent Kinetic Energy," *AIAA Journal*, Vol. 8, No. 8, Aug. 1970, pp. 1508–1510.

[2] Lee, S. C. and Harsha, P. T., "The Use of Turbulent Kinetic Energy in Free Mixing Studies," *AIAA Journal*, Vol. 8, No. 6, June 1970, pp. 1026–1032.

[3] Bradshaw, P., Ferriss, D. H., and Atwell, N. P., "Calculation of Boundary Layer Development Using the Turbulent Energy Equation," *Journal of Fluid Mechanics*, Vol. 28, Pt. 3, 1967, pp. 593–616.

[4] Laster, M. L., "Inhomogeneous Two-Stream Turbulent Mixing Using the Turbulent Kinetic Energy Equation," TR 70-134, May 1970, Arnold Engineering Development Center, Tenn.

[5] Patankar, S. V. and Spalding, D. B., "A Finite-Difference Procedure for Solving the Equations of the Two-Dimensional Boundary Layer," *International Journal of Heat and Mass Transfer*, Vol. 10, No. 10, Oct. 1967, pp. 1389–1411.

[6] Forstall, W., Jr., "Material and Momentum Transfer in Coaxial Gas Streams," D.Sc. thesis, May 1949, MIT, Cambridge, Mass.

[7] Prandtl, L., "Bemerkungen zur Theorie der freien Turbulenz," *Zeitschrift fur Angewandte Mathematik und Mechanik*, Vol. 22, No. 5, Oct. 1942, pp. 241–243.

[8] Peters, C. E., "Turbulent Mixing and Burning of Coaxial Streams Inside a Duct of Arbitrary Shape," TR 68-270, Jan. 1969, Arnold Engineering Development Center, Tenn.

[9] Paulk, R. A., "Experimental Investigation of Free Turbulent Mixing of Nearly Constant Density Coaxial Streams," M.S. thesis, March 1969, University of Tennessee, Knoxville, Tenn.

[10] Peters, C. E., Chriss, D. E., and Paulk, R. A., "Turbulent Transport Properties in Subsonic Coaxial Free Mixing Systems," AIAA Paper 69-681, San Francisco, Calif., 1969.

[11] Chriss, D. E., "Experimental Study of the Turbulent Mixing of Subsonic Axisymmetric Gas Streams," TR 68-133, Aug. 1968, Arnold Engineering Development Center, Tenn.

Self-Correcting Initial Value Formulations in Nonlinear Structural Mechanics

JAMES A. STRICKLIN* AND WALTER E. HAISLER†
Texas A&M University, College Station, Texas
AND
WALTER A. VON RIESEMANN‡
Sandia Corporation, Albuquerque, N. Mex.

Introduction

THE purpose of this Note is to explore the initial value formulation for nonlinear static structural mechanics problems. It is assumed that the nonlinearities are due to small plastic strains and/or large deflections.

Probably the most widely used methods for nonlinear structural analysis by the finite element approach are the incremental procedure of Turner, Dill, Martin and Melosh[1] for large deflections and the tangent stiffness method of Pope[2] for plastic strains. In either case, the incremental procedure requires that new stiffness matrices be computed and "inverted" at each load increment and, consequently, requires the expenditure of large amounts of computer time. Until recently, however, the incremental and Newton-Raphson approaches were the only methods capable of solving for highly nonlinear behavior. In this Note, an alternative approach, a self-correcting initial value formulation, is presented which may be used to solve for highly nonlinear behavior. The method is demonstrated by solving for the geometrically nonlinear behavior of a single degree-of-freedom system and for the deflection of a spherical cap under a point load at the apex.

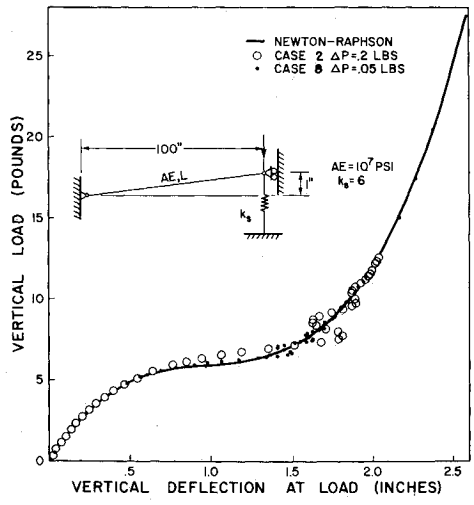

Fig. 1 Load deflection curve for truss.

Initial Value Formulation

The analysis of nonlinear problems by either the finite element method or the finite difference method gives rise to the set of equations:

$$[K]\{q\} = P\{\bar{P}\} + \{Q\} \tag{1}$$

where $[K]$ = linear stiffness matrix, $\{q\}$ = generalized displacements, $P\{\bar{P}\}$ = generalized forces due to applied external loads, P = convenient normalizing factor, $\{Q\}$ = pseudo generalized forces due to nonlinearities and dependent on the displacements.

Taking the derivative of Eq. (1) with respect to the scalar P yields

$$[K]\{\dot{q}\} = \{\bar{P}\} + \{\dot{Q}\} \tag{2}$$

where a dot indicates differentiation with respect to P.

Equation (2) is one form which has been solved. By using chain rule differentiation on $\dot{Q}$, another form of Eq. (2) is obtained.

$$\{\dot{Q}\} = [K^*]\{\dot{q}\} \tag{3}$$

where the elements of K^* are given by

$$k_{ij}^* = \partial Q_i/\partial q_j$$

Substituting Eq. (3) into Eq. (2) yields the equation

$$([K] + [K^*])\{\dot{q}\} = \{\bar{P}\} \tag{4}$$

The solution of Eqs. (2) and (4) which tends to drift away from the correct solution may be corrected by adding, to either Eq. (2) or (4), the unbalance of force f given by

$$\{f\} = -[K]\{q\} + P\{\bar{P}\} + \{Q\} \tag{5}$$

Multiplying Eq. (5) by an arbitrary factor Z and adding the result to the righthand side of Eqs. (2) and (4) yields:

$$[K](\{\dot{q}\} + Z\{q\}) = (1 + ZP)\{\bar{P}\} + Z(\{Q\} + \{\dot{Q}\}1/Z) \tag{6}$$

$$([K] + [K^*])\{\dot{q}\} + Z[K]\{q\} = (1 + ZP)\{\bar{P}\} + Z\{Q\} \tag{7}$$

Equations (6) and (7) are self-correcting first-order differential equations and to the author's knowledge have not been presented previously. If $Z = 1.0$ and an Euler forward

Table 1 Single degree-of-freedom studies[a]

Case	$Z(P)^{1/2}$	ΔP	Maximum load, lb	Comment
1	224	0.2	79	Numerically unstable
2	112	0.2	264	Numerically unstable
3	56	0.2	870	Numerically unstable
4	56	0.2	>1160	Stable
5	632	0.1	142	Numerically unstable
6	316	0.1	>600	Stable
7	1789	0.05	>300	Stable
8	894	0.05	>300	Stable

[a] $C = Z^{0.2}/2$ except for Case 4 where $C = 0.2\ (\Delta P)Z$.

Received March 17, 1971; revision received May 21, 1971. Research supported by Sandia Contract 82-5617 and NASA Grant NGL-44-011-044 and by the United States Atomic Energy Commission.

Index category: Structural Static Analysis.

* Professor, Department of Aerospace Engineering. Member AIAA.

† Assistant Professor, Department of Aerospace Engineering. Associate Member AIAA.

‡ Member, Technical Staff. Member AIAA.